Journal of Materials Chemistry C

Accepted Manuscript

This is an *Accepted Manuscript*, which has been through the RSC Publishing peer review process and has been accepted for publication.

Accepted Manuscripts are published online shortly after acceptance, which is prior to technical editing, formatting and proof reading. This free service from RSC Publishing allows authors to make their results available to the community, in citable form, before publication of the edited article. This *Accepted Manuscript* will be replaced by the edited and formatted *Advance Article* as soon as this is available.

To cite this manuscript please use its permanent Digital Object Identifier (DOI®), which is identical for all formats of publication.

More information about *Accepted Manuscripts* can be found in the **Information for Authors**.

Please note that technical editing may introduce minor changes to the text and/or graphics contained in the manuscript submitted by the author(s) which may alter content, and that the standard **Terms & Conditions** and the **ethical guidelines** that apply to the journal are still applicable. In no event shall the RSC be held responsible for any errors or omissions in these *Accepted Manuscript* manuscripts or any consequences arising from the use of any information contained in them.

RSC Publishing

www.rsc.org/materialsC

Registered Charity Number 207890

Journal of
Materials Chemistry C

RSCPublishing

PAPER

Cite this: DOI: 10.1039/x0xx00000x

Blue phases induced by rod-shaped hydrogen-bonded supermolecules possessing no chirality or mesomorphic behaviour

Yingyi Li, Yuehua Cong, Huishu Chu and Baoyan Zhang*

DOI: 10.1039/x0xx00000x

www.rsc.org/

A liquid crystalline compound containing (-)-menthol as chiral centre was prepared and used as host material, which liquid crystalline behaviours were investigated. The host did not exhibit any blue phase on heating and cooling. A series of conventional rod-shaped hydrogen-bonded supermolecules with different terminal chain lengths were synthesized and used as dopants. These supermolecules did not possess chirality or exhibit any mesomophic behaviour. By adding proton acceptor, proton donor and supermelcules into the host liquid crystal, respectively, the effects of these dopants on the liquid crystalline properties of mixtures were studied. Formation of blue phases was induced by adding supermolecules into host liquid crystal. The widest temperature range of blue phase was about 45K.

Introduction

The study of blue phase (BP) is one of the most interesting areas in liquid crystal science.[1-3] BPs generally exist between isotropic (Iso) and chiral nematic (N*) phases.[4] BPs are classified as BPI, BPII and BPIII.[5,6] While BPIII is amorphous, BPII and BPI have simple cubic and body-centred cubic structures, respectively. BPII and BPI have three dimensional cubic lattices, in which the directors from double twist cylinders are stabilized by disclinations.

BPs have several advantages in optical isotropy and fast respond speed,[7,8] however they usually exist in a narrow temperature range, which limits their potential applications. Hence stabilization of BPs has attracted much research interests. Several approaches have been used to improve BPs stability and therefore extend the useful temperature range. Among the approaches of BP stabilization, besides polymer stabilization[9,10] and nano-doping method,[11] low-molecular weight approaches are widely reported.[12,13] A hydrogen bonded complex with wide BP range (23 K) was reported by Yang's group.[14] Coles *et al.* reported that dimeric chiral molecules possessing a high flexoelecticity coefficient exhibited a wide temperature range of BP from 60 to 16 ℃ (about 44K).[15] Besides, several unconventional shaped low-weight molecules, such as U-shaped, T-shaped and bent-core molecules, were synthesized for stabilization of BP. Yoshizawa *et al.* reported that a binaphthyl derivative (U-shaped) possessing wide temperature range of BP exhibited an isotropic-BP-smectic phase sequence.[16] They also reported a chiral T-shaped compound with a wide temperature range of BP (more than 10 K) on cooling.[17] A biaxial bent-core molecule, reported by Choi's group, exhibited BPI which was more than 15 K.[18] In addition to above unconventional shaped molecular designs, more recently, Kishikawa *et al.* reported that the temperature range of BP can be expanded by mixing achiral homologues in simple rod-like monoester compounds.[19]

However, reported additives of BP stabilization are generally required to possess high chirality, proper melting point, proper liquid crystalline temperature range and well compatibility, which limit the choice of additives. It's well known that hydrogen-bonded self-assembled supramolecular liquid crystal has dynamic reversible features and special response characteristics to environmental stimuli.[20,21] In this paper, we investigate the possibility to generate BP by doping a host liquid crystal, that do not exhibit BP, merely with hydrogen bonded self-assembled supermolecules that do not exhibit any mesomorphic behaviour are neither chiral nor unconventional shaped. This study provides a feasible and effective approach for formation and stabilization of BP.

Results and discussion

A rod-shaped chiral compound 4-(Menthyloxy acetoxy)phenyl-4'-(undec-10-enoyloxyphenyldiazenyl) benzoate (**M**) was used as host material. Mesogenic core of **M** was a *trans*-azobenzene that bridged a flexible olefinic chain, containing one double bound, with the menthyl chiral centre. The chemical structure of **M** is shown as Fig. 1(a). The dopant supermolecules were formed by a pyridyl-containing pyridin-4-yl 4-(allyloxy) benzoate (**PAB**) (Fig. 1(b)) and one of following acids: octanoic acid (**8A**), decanoic acid (**10A**), dodecanoic acid (**12A**)

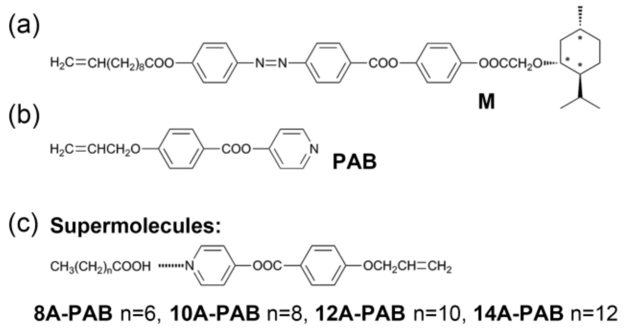

Fig. 1 Chemical structures of **M**, **PAB** and **supermolecules**.

and tetradecanoic acid (**14A**) (Fig. 1(c)) connected by self-assembled hydrogen-bonds. The details of synthesis and characterisation of the above mentioned compounds are shown in Electronic Supplementary Information (ESI).

Investigation of the physical properties of M, PAB and supermolecules

The thermal properties of **M**, **PAB** and supermolecules **8A-PAB**, **10A-PAB**, **12A-PAB**, **14A-PAB** were obtained from a TA Q2000 differential scanning calorimeter (DSC) and a ZEISS Axio Scope A1 pol polarizing optical microscope (POM) equipped with a Linkam THMSE-600 hot stage. The phase transition temperatures, corresponding enthalpy changes and mesophase types are listed in Table 1, which were obtained on the second heating and cooling scans. Fig. 2 shows the representative DSC curves of **M**, **PAB** and **10A-PAB**.

Table 1 Thermal properties of **M**, **PAB** and supermolecules

Compounds	Mesophase, phase transition temperature (℃) and enthalpy changes ($J\ g^{-1}$)
M	Heating: Cr 92.3 (37.51) SmC* 115.7 (0.53) N* 152.5 (0.37) Iso Cooling: Cr 60.4 (-46.73) SmC* 112.6 (-0.47) N* 151.7 (-0.62) Iso
PAB	Heating: Cr 135.2 (44.34) Iso Cooling: Cr 114.0 (-46.77) Iso
8A-PAB	Heating: Cr 155.2 (48.24) Iso Cooling: Cr 147.7 (-38.70) Iso
10A-PAB	Heating: Cr 146.0 (47.70) Iso Cooling: Cr 137.6 (-36.31) Iso
12A-PAB	Heating: Cr 130.3 (42.47) Iso Cooling: Cr 115.2 (-48.63) Iso
14A-PAB	Heating: Cr 108.2 (34.24) Iso Cooling: Cr 81.0 (-36.53) Iso

The DSC curves of **PAB**, **8A-PAB**, **10A-PAB**, **12A-PAB** and **14A-PAB** exhibited only an endothermic peak in heating process and an exothermic peak in cooling process, respectively. The corresponding observations of POM also suggested that these compounds did not exhibit any mesomorphic behaviour.

The DSC curve of **M** showed three reversible phase transitions. And the phase transitions were further investigated by a X-ray diffractometer (Bruker D8). Fig. 3 indicates the X-ray diffraction (XRD) patterns of **M** at 105 and 135 ℃, respectively. The pattern showed a sharp peak at $2\theta \approx 2.4°$ (*d*-spacing 36.81 Å) and a diffused peak at $2\theta \approx 18.6°$ (*d*-spacing 4.77 Å) at 105 ℃. The sharp peak in the small-angle region is characteristic of smectic structures while the diffused peak indicates the lateral packing. MM2 calculation's method gave a theoretical molecular length of **M** 39.99 Å. The tested *d*-spacing was less than the molecular length, suggesting a titled smectic molecular arrangement. Therefore the liquid crystalline phases at 60.4~112.6 ℃ on cooling and 92.3~115.7 ℃ on heating were determined to be chiral smectic C (SmC*) phases. The XRD pattern at 135 ℃ showed only a diffused peak at $2\theta \approx 19.3°$ (*d*-spacing 4.60 Å). For this phase, broken focal conic textures were observed by POM (Fig. S3), therefore the liquid crystalline phase at 112.6~151.7 ℃ on cooling and 112.6~152.5 ℃ on heating was assigned as chiral nematic (N*) phase. The three exothermic peaks on cooling from high to low temperature in order represented as: an Iso to N* phase transition ($T_{\text{Iso-N*}}$), a N* to SmC* phase transition ($T_{\text{N*-SmC*}}$), and a SmC* to crystallization (Cr) phase transition ($T_{\text{SmC*-Cr}}$), respectively. And the phase transitions were consistent with the observations by POM.

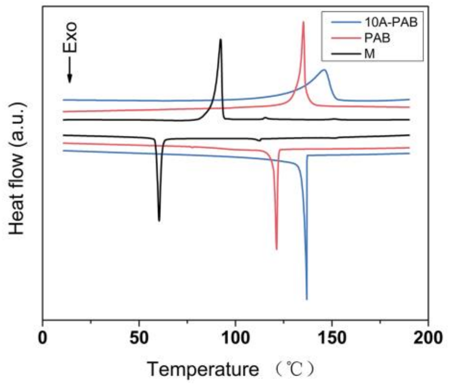

Fig. 2 DSC curves of **M**, **PAB** and **10A-PAB**.

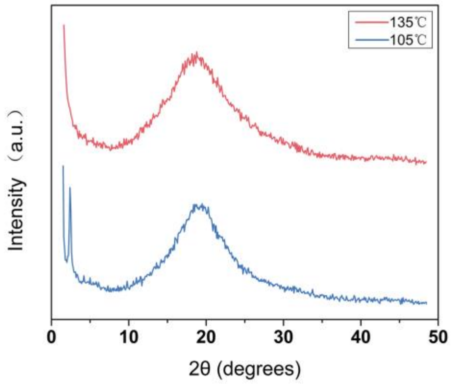

Fig. 3 X-ray diffraction profiles of **M** at 105 ℃ (in blue) and at 135 ℃ (in red).

Investigation of FT-IR and 2D-IR correlation spectroscopies

Only the proton donor and the proton acceptor were steadily connected by hydrogen bond in a certain temperature range, it can be determined that the changes of liquid crystalline properties of mixtures were induced by supermolecules, not the sum of influences by proton donors and proton acceptors.

Fourier transform infrared (FT-IR) spectroscopy is well suited for such investigation of hydrogen-bonded interaction between the carboxylic acid and the pyridyl fragments. Transmission FT-IR spectra at various temperatures were measured in KBr solid using PerkinElmer spectrum One (B) spectrometer with a resolution of 2 cm^{-1}. The temperature-dependent FT-IR spectra were measured at intervals of 2 ℃ over a temperature range from 40 to 166 ℃.

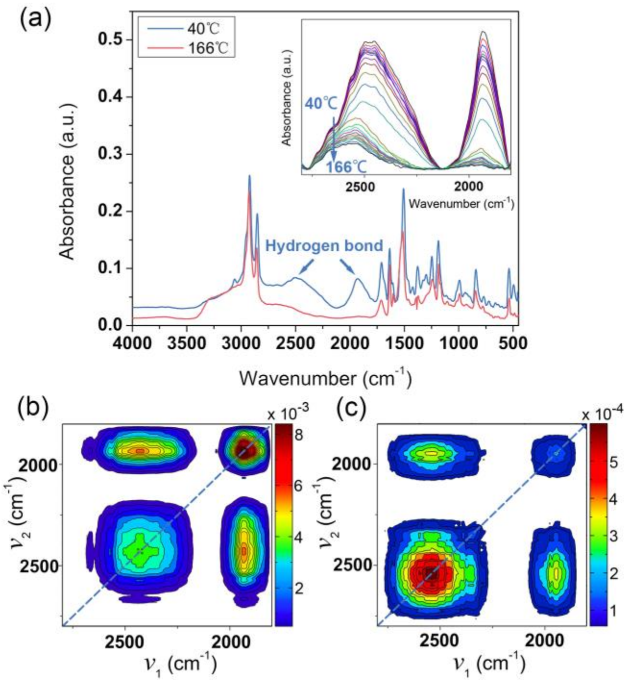

Fig. 4 (a) FT-IR spectra of **10A-PAB** at 40 ℃ (in blue) and 166℃ (in red). The insert indicates the FT-IR spectra from 40 to 166 ℃ in the 2800-1800 cm^{-1} region. (b) 2D-IR correlation synchronous spectra at 40-50 ℃ in the 2800-1800 cm^{-1} region. (c) The corresponding 2D-IR correlation synchronous spectra at 156-166 ℃.

As shown in Fig. 4(a), the FT-IR spectra of **10A-PAB** at 40 ℃ indicated two broad absorption bands centred at 2482 and 1931 cm^{-1}, which were assigned to hydrogen-bonding interaction between the carboxylic acid and the pyridyl fragments. The absorption band showed a wavenumber-upshift with an increase of temperature, accompanied with a decrease of absorbance. When the temperature was up to 166 ℃, the hydrogen bonding absorption bands moved to 2612 and 1941 cm^{-1}. The insert gives the temperature-dependent FT-IR spectra of **10A-PAB** in the region from 2800 to 1800 cm^{-1}.

Two-dimensional infrared (2D-IR) correlation spectroscopy intensities were acquired from a MATLAB program by analysing the corresponding temperature-dependent IR spectra, and the 2D correlation method was proposed by Noda.[22,23] 2D-IR correlation spectroscopy is a powerful tool to provide more visual and legible spectral information for confirming the existence of hydrogen bond and analysing its changes with temperature. According to Noda's rule, the diagonal peak in the synchronous spectra is the result of the autocorrelation of the perturbation-induced dynamic variations of IR spectra, which is called auto-peak. Aside from diagonal auto-peaks, off-diagonal peaks are called cross-peaks. A positive cross-peak suggests that the intensities of groups decrease or increase simultaneously under external perturbation. A negative cross-peak indicates opposite band intensity changes. More specifically, one band intensity decreases, the other increases simultaneously.

Fig. 4(b) depicts counter plots of 2D-IR correlation synchronous spectra in the region from 2800 to 1800 cm^{-1}, which were constructed from the temperature-dependent IR spectra between 40 and 50 ℃. Two obvious diagonal peaks were shown in the 2D-IR correlation synchronous spectra in the 2800-1800 cm^{-1} region. One peak was at 2482 cm^{-1} and the other one was at 1931 cm^{-1}. The corresponding patterns of cross-peaks were positive, which represented the simultaneous decrease of intensities of absorption bands.

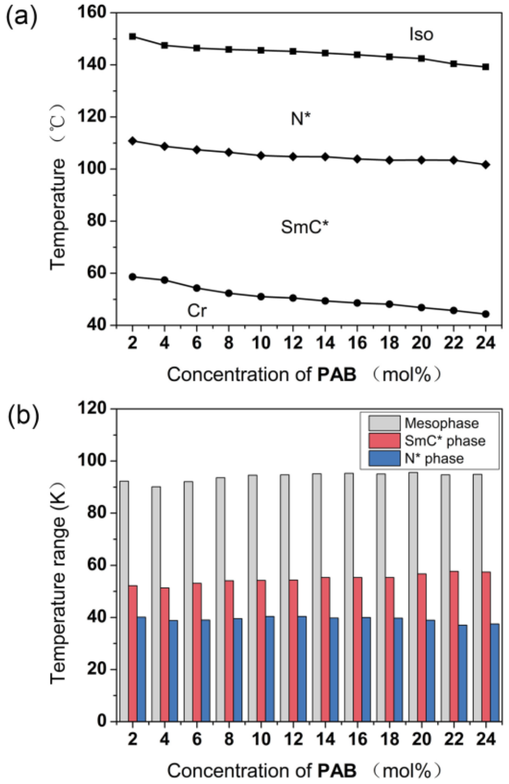

Fig. 5 (a) Phase diagram of the mixtures of **M** and **PAB** against the concentration of **PAB**. (b) Temperature ranges of SmC* phase, N* phase and the whole mesophase of mixtures in **M/PAB** series.

The corresponding 2D-IR correlation synchronous spectra between 156 and 166 ℃ were analysed in the same method (Fig. 4(c)). As mentioned above, the absorption band of FT-IR at 1941 cm^{-1} became less obvious when the temperature was up to 166 ℃. However, in the 2D-IR correlation synchronous spectra, an obvious atuo-peak was shown at 1941 cm^{-1}, and the corresponding positive cross-peaks indicated that the intensity decreased on heating process from 156 to 166 ℃. Therefore, it was inferred that the absorption band at 1941 cm^{-1} still steadily existed when the temperature was lower than 156℃. In this paper, the clear points of all samples were lower than 156℃, so when the samples were in mesophase the proton donors and acceptors were connected by hydrogen bonds in supramolecular forms.

Effect of dopants on the thermal properties of mixtures

PAB, the four different acids and the range of supermolecules as dopants were added into **M** with different molar ratios, respectively. To avoid phase separation phenomenon, the maximum amount of dopant was 24 mol%. The effect of the dopants on thermal properties of mixtures was investigated, which inclued the influences on phase transition temperatures and temperature ranges of each liquid crystalline phases.

M plus **PAB**

Calculating by weight, the maximum mass fraction of **PAB** in

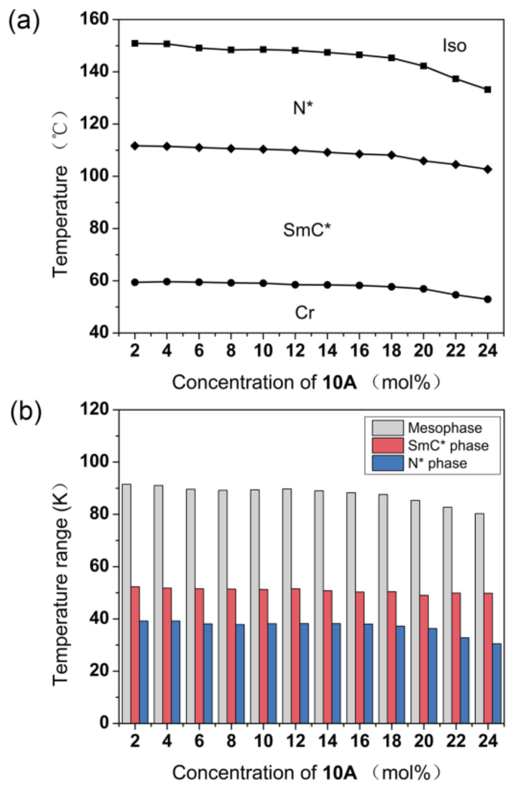

Fig. 6 (a) Phase diagram of the mixtures of **M** and **10A** against the concentration of **10A**. (b) Temperature ranges of SmC* phase, N* phase and the whole mesophase of mixtures in **M/10A** series.

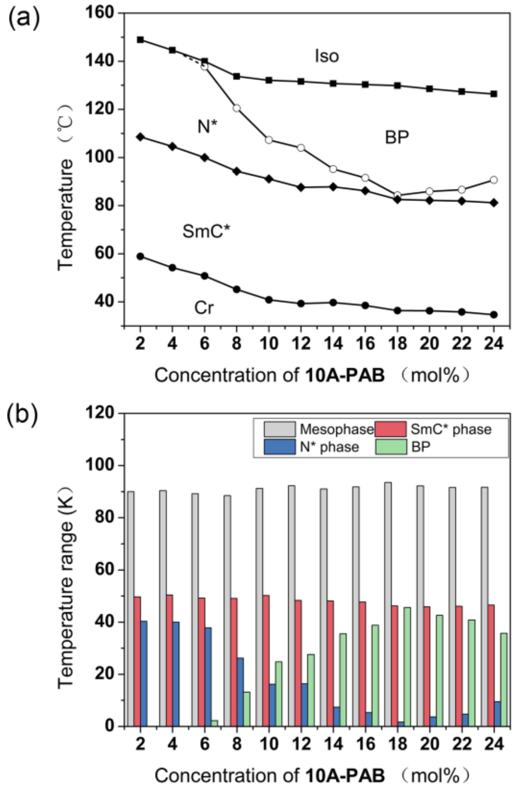

Fig. 7 (a) Phase diagram of the mixtures of **M** and **10A-PAB** against the concentration of **10A-PAB**. (b) Temperature ranges of SmC* phase, N* phase, blue phase and the whole mesophase of mixtures in **M/10A-PAB** series.

mixture was 10.4 wt%. The Iso-N*-SmC*-Cr phase sequence was observed in cooling process. The only observable effect of **PAB** was a slight decrease of the phase transition temperatures $T_{Iso\text{-}N*}$, $T_{N*\text{-}SmC*}$ and $T_{SmC*\text{-}Cr}$ (Fig. 5(a)). The maximum decrease effect was observed for the mixture **M(76mol%)/PAB(24 mol%)** with $T_{Iso\text{-}N*}$ $T_{N*\text{-}SmC*}$ $T_{SmC*\text{-}Cr}$ dropping by 11.7, 9.1 and 14.3 K, respectively.

The whole mesophases of the above-mentioned mixtures included N* and SmC* phases. Fig. 5(b) indicates the influence of **PAB** content on the temperature ranges of N* phase, SmC* phase and the whole mesophase. A less pronounced effect was observed for the changes of temperature range of N* phase and that of SmC* phase, which were also only limited within several degrees. The above results suggested that the formation of BP could not be induced by only doping proton acceptor **PAB** in **M**.

M plus acids

In order to study the effect of monoacid contents on the thermal properties of mixtures, monoacids were added into **M** with different proportions. All the tested acids gave similar results. Decanoic acid (**10A**) was described as an example. The maximum mass fraction of **10A** in mixture was 7.2 wt%.

Fig. 6(a) indicates the phase diagram against the concentration of **10A** in mixtures. Similar to **PAB**, the addition of acids did have no major effect on the phase transition sequences of mixtures with a small decrease of $T_{Iso\text{-}N*}$, $T_{N*\text{-}SmC*}$ and $T_{SmC*\text{-}Cr}$ decreased 17.7K (from 150.9 to 133.2 ℃)，9.0K (from 111.7 to 102.7℃) and 6.5K (from 59.4 to 52.9℃) with the increase of percentage of acid.

Fig. 6(b) shows the influence of content change of **10A** on the temperature ranges of N* phase, SmC* phase and the whole mesophase. The content change of **10A** did not influence the temperature range of SmC* phase obviously. Temperature range of N* phase and the whole mesophase decreased gradually with the increase of the concentration of **10A**, but only within several degrees. From the above investigation, only adding proton donor **10A** into **M** did not induce the formation of BP.

M plus **10A-PAB**

The phase diagram against the concentration of supermolecule **10A-PAB** is shown as Fig. 7(a). When **M** was doped with 2 mol% and 4 mol% of **10A-PAB**, the only detected effect was a decrease of phase transition temperatures. As the amount of dopant reached 6 mol%, a blue phase formed between Iso and N* phases. With the increase of content of supermolecule, the phase transition temperatures $T_{Iso\text{-}BP}$, $T_{N*\text{-}SmC*}$ and $T_{SmC*\text{-}Cr}$ decreased gradually, $T_{BP\text{-}N*}$ decreased first and then increased.

The temperature range at which the BP existed increased with the amount of dopant reaching the maximum of 45.6 K at 18 mol% of **10A-PAB** (Fig. 7(b)). The temperature range at which the whole mesophase existed did not change obviously with the increase of **10A-PAB** however a general shift toward narrower temperature range was observed. Interestingly the BP formation did not affect the temperature range of SmC* phase but replaced N* phase.

Effect of chain length on BP

In order to further investigate the chain length on the BP, **M** was doped with **8A-PAB**, **12A-PAB** and **14A-PAB** in different mole fractions, respectively. Figs. 8(a-c) indicate phase diagrams of

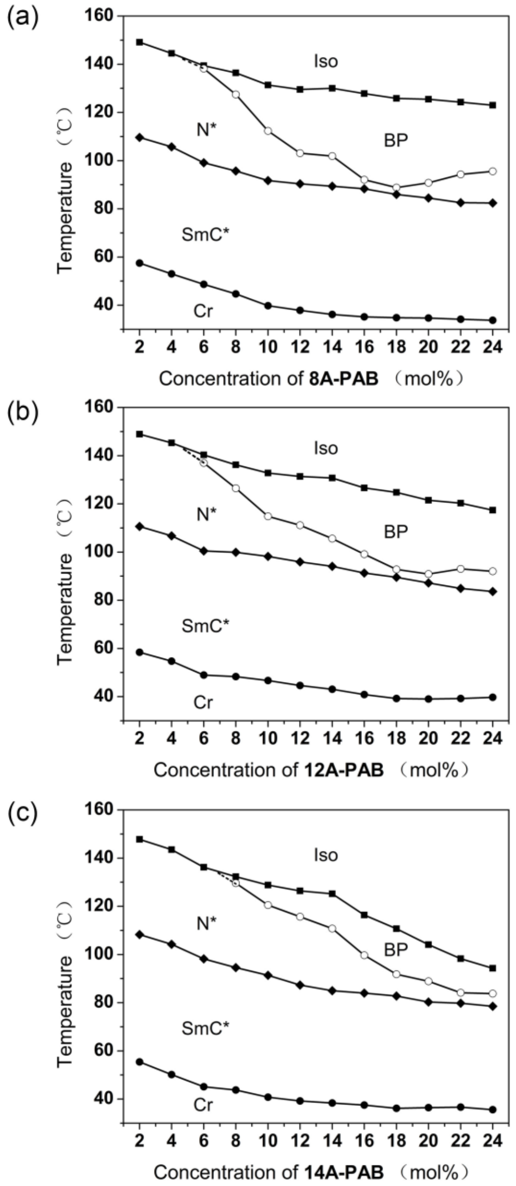

Fig. 8 Phase diagrams of the mixtures in **M/8A-PAB** series (a), in **M/12A-PAB** series (b) and in **M/14A-PAB** series (c).

M/8A-PAB, **M/12A-PAB** and **M/14A-PAB** series against the concentration of supermolecules, respectively. The effects of each homologues on phase transitions are similar as that of **10A-PAB**. Fig. 9 indicates the temperature ranges of BPs of all mixtures in this paper. The mixtures not possessing blue phase are marked as black squares. The least amounts of supermolecules that induced the formations of BP in series of **M/8A-PAB**, **M/10A-PAB**, **M/12A-PAB** and **M/14A-PAB** were 6, 6, 6 and 8 mol%, which were 3.5, 3.8, 4.0 and 5.9 wt% in mass fraction, respectively. The results suggested that just adding a small amount of supermolecules into **M** can induce the formations of BPs.

The effect of monoacid carbon chain length on temperature range of BP was studied by comparing the mixtures containing the same supramolecular content in each series. Taking the mixtures containing 18 mol% of supermolecules as representative examples, the BP ranges of **M(82mol%)/8A-PAB(18mol%)**, **M(82mol%)/10A-PAB(18mol%)**, **M(82mol%)/12A-PAB(18 mol %)** and **M(82 mol%)/14A-PAB(18mol %)** were 39.0, 45.6, 32.0 and 18.9 K, respectively. With an increase of the length of monoacid carbon chain, the temperature range of BP became wider first and then narrower. And the mixture using decanoic acid as proton donor in supermolecule showed the widest BP range. When the mixtures were doped with other mole fractions of supermolecules, the effect of the length of monoacid carbon chain on temperature range of BP was also proved.

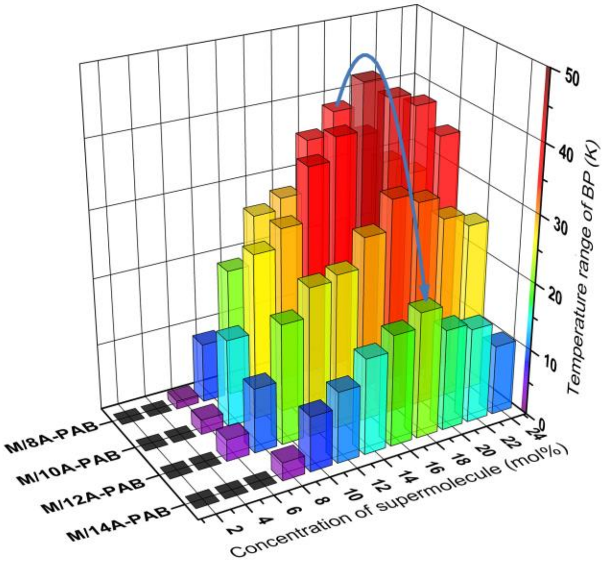

Fig. 9 Temperature ranges of the BP of all mixtures in this paper. The samples that do not exhibit BP are marked with black squares in figure. Different colours represent different temperature ranges of BP.

Investigation of the optical texture and the selective reflection

The optical textures of the mixture **M (82mol%)/10A-PAB(18mol%)** was analysed by POM during slow cooling (0.2 ℃/min) from 130 to 40 ℃ in transmissive and reflective mode (Figs. 10(a-d)).

Figs. 10(a, b) indicate the platelet textures of BP. When the temperature was slightly below $T_{\text{Iso-BP}}$, the platelet textures under transmissive mode could not be easily analysed, therefore they were investigated in reflective mode using the same brightness of light of POM (Fig. 10(a)). Fig. 10(b) was obtained in transmissive mode. With the decrease of temperature, the reflective colour of platelets showed an obvious redshift, which was caused by the Bragg reflection from the (110) plane in body-centred cubic structure of BPI. This redshift phenomenon of BPI with the decrease of temperature was also reported before.[15] Figs. 10(c, d) show the focal conic and fan-shaped textures of **M (82mol%)/10A-PAB(18mol%)** in N* and SmC* phases, respectively.

Central wavelengths of the reflection spectra of the mixture **M(82mol%)/10A-PAB(18mol%)** produced at different temperatures are shown as Fig. 11(a). The specific reflection spectra are shown as Fig. S4(a). A UV/vis/NIR spectrometer (PerkinElmer 950) was used to measure the reflection wavelength. The temperature was controlled by a cool and hot stage (Linkam THMSE-600). The cooling rate was also 0.2 ℃/min. In a very narrow temperature region which was slightly lower than $T_{\text{Iso-BP}}$, the reflective peaks shifted from a short wavelength to a long one. A 84 nm wavelength red-shift (from 575 to 659 nm) was observed with a decrease of temperature. The maximum wavelength was at ~659 nm.

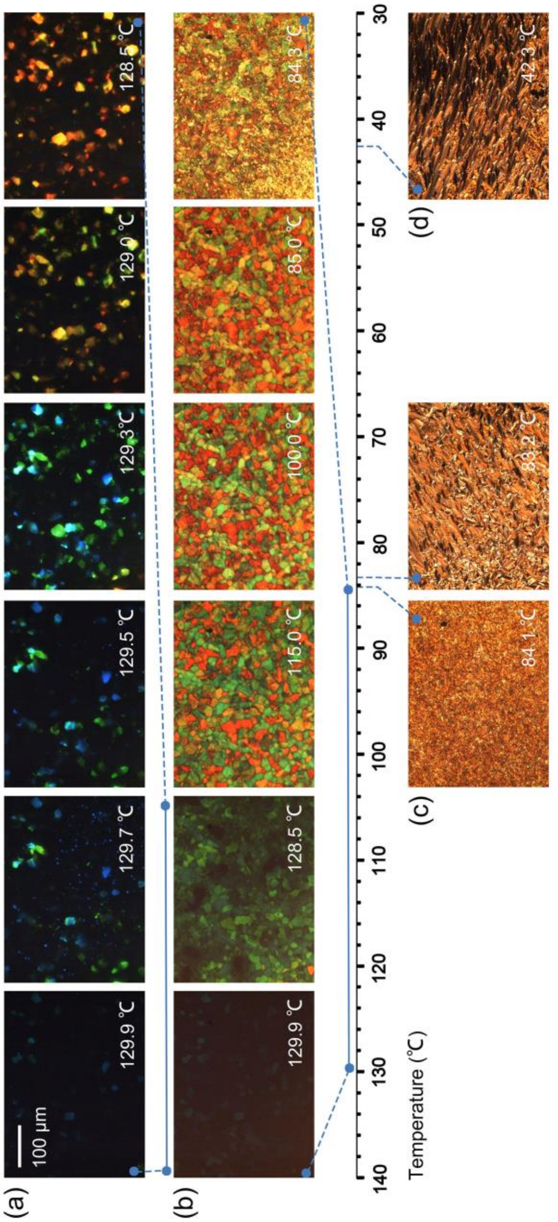

Fig. 10 The optical textures of the mixture **M(82mol%)/10A-PAB(18 mol%)** at indicated temperatures by POM.

On further cooling, the reflection wavelength gradually decreased by 12 nm (from 659 to 647 nm) until the N* phase was reached. It is well-known that the reflection wavelength of BPI changes obviously with temperature, but there is a negligible or at best a weak variation in BPII.[24] The reflection peaks showed during on slowly cooling cycle were assigned as the Bragg diffraction from (110) plane of the cubic lattice in BPI. In addition, at the BPI to N* phase transition, the reflection wavelength exhibited a discontinuous change from 647 to 492 nm. The trend of the reflection spectra corresponded to the above mentioned optical texture behaviours.

Fig. 11(b) displays photographs of **M(82mol%)/10A-PAB(18 mol%)** at the indicated temperatures, which were taken after keeping at the target temperature for a few minutes. In order to observe the reflective colour of the sample more obviously, a black super thin glass was used as bottom. The reflection spectra at 129.5, 95.5 and 83.0 ℃ are shown as Figs. S4(b)(c)(d).

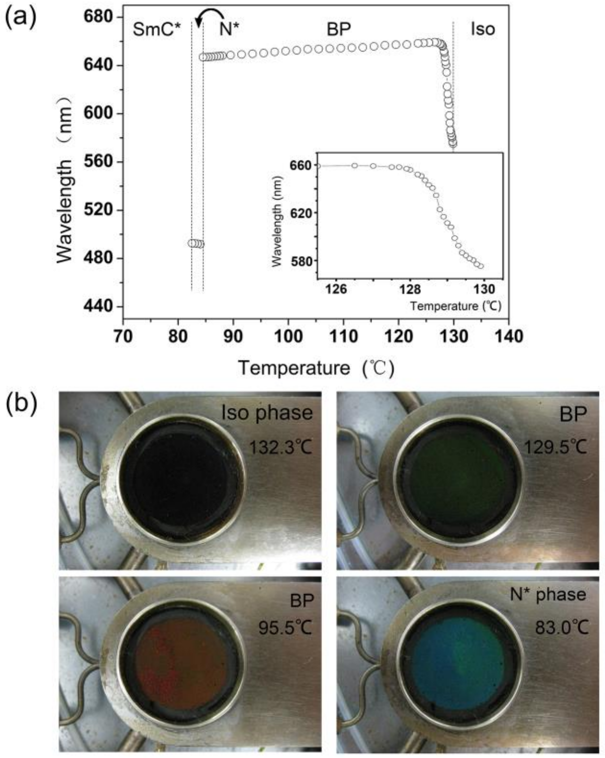

Fig. 11 (a) Temperature dependence of reflection wavelength of the mixture **M(82mol%)/10A-PAB(18mol%)**. The insert is the magnified one. (b) Photographs of the mixture **M(82mol%)/10A-PAB(18mol%)** on hot stage at the indicated temperatures.

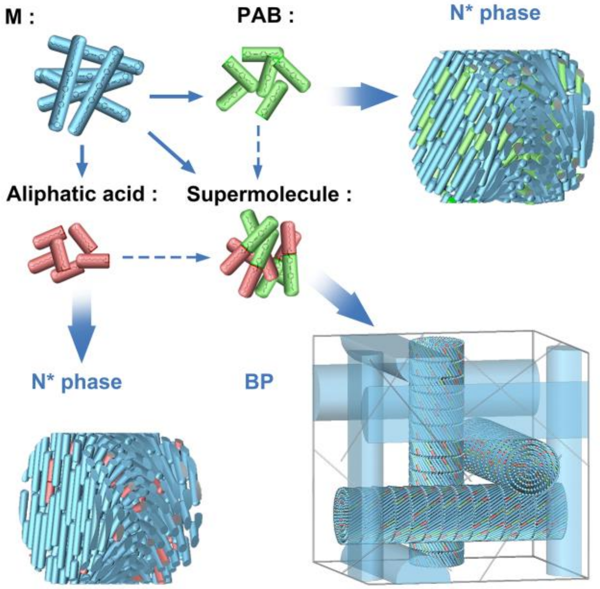

Fig. 12 Schematic representation of the arrangement of mixtures with different dopants.

Discussion of the BP formation mechanism by hydrogen-bonded supermolecule

We discuss the formation of BPs as the following mechanism. It is well-known that BP only appears in the chiral system. The dopants used in this paper possess no chirality, while the host material (**M**) is a chiral rod-shaped liquid crystalline compound. Helical twisting power (HTP) was measured using the Cano

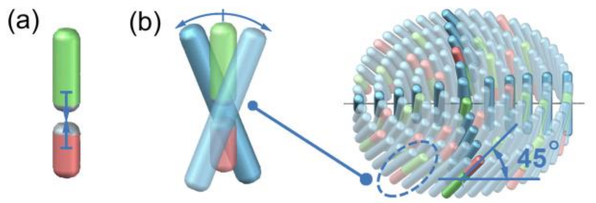

Fig. 13 (a) Schematic representation of hyrogen bondeding supermolecule. (b) The estimated arrangement of adjacent molecules as supermolecules are doped into host material. By intermolecular interaction the molecules form a double twisted arrangement.

wedge method at room temperature. The HTP of **M** was 5.0 μm^{-1}. In the cooling process, **M** did not possess blue phase but form N* phase as the temperature was lower than isotropic phase. Comparing the molecular arrangement in BP with that in N* phase, the structures are double-twisted and single-twisted, respectively. As the illustration in Fig. 12, when **M** was doped with chiral accepter or donor, BP did not appear in the cooling process from Iso phase. While **M** was doped with supermolecule, in other words, the proton donor and accepter were added into **M** simultaneously, cubic BP was formed on the cooling cycle. It can be inferred that the hydrogen bonding supermolecule played an inducing role in the formation of cubic BP. In addition, the dopants did not possessing chirality, and did not exhibit any mesomorphic behaviour. Therefore, for dopants, the chirality and liquid crystallinity are not the essential factors in the formation of BP.

In other publications, the cubic BPs induced by the unconventional shaped molecules have been successfully explained. The results in these papers suggested that the intermolecular twist contribute the formation of BP. In this paper, the supermolecule was connected by hydrogen bond, which is an intermolecular force and stronger than van der Waals force. Unlike a covalent bond, there is no electron cloud in the hydrogen bond possessing a certain bond length and directionality. The adjacent parallel molecules make a twisted rotation by squeezing the hydrogen bonds. Then the double-twisted cylinders are formed through the interaction of molecules, which are stabilized by disclinations. Above all, we postulate that adding supermolecules into **M** promotes the generation of intermolecular twist (Fig. 13), which is an important factor in the formation of BP. By replacing **10A-PAB** with its homologues, the supramolecular induced blue phases were further proved in the results.

Conclusions

A cubic BP induced by adding supermolecules into a chiral liquid crystalline host was described. The synthesised liquid crystalline compound did not exhibit BP either in heating or cooling progress. The effects of dopants, such as proton donor, proton acceptor and supermolecule, on the liquid crystalline properties of the mixtures were investigated. The results indicated that the supermolecule played an inducing role in the formation of BP. Interestingly, the supermolecules did not exhibit any mesomorphic behaviour or chirality. It suggested that, for dopants, chirality and liquid crystallinity are not essential factors in the formation of BP. The widest temperature range of BP in this paper was about 45 K, suggesting that there was an obvious effect on stabilization of BP by doping with hydrogen bonded self-assembled supermolecules. The hypothesis of BPs stabilisation mechanism by hydrogen bonding supramolecular dopants was discussed and tested by adding different supramolcular homologues into host liquid crystal. The inducing role of supermolecules in the formation of BPs was proved.

Acknowledgements

The authors are grateful to National Science Fundamental Committee of China, and HI-Tech Research and development program (863) of China.

Notes and references

Centre for Molecular Science and Engineering, Northeastern University, Shenyang, 110004, Liaoning, People's Republic of China. Fax: +86-24-83687446 E-mail: baoyanzhang@hotmail.com

† Electronic Supplementary Information (ESI) available: [Synthesis and spectral data of **M**, **PAB** and supermolecules, and reflection spectra of **M(82mol%)/10A-PAB(18mol)**.]. See DOI: 10.1039/b000000x/

1 W. Y. Cao, A. Munoz, P. Palffy-Muhoray and B. Taheri, *Nat. Mater.*, 2002, **1**, 111-113.
2 G. Heppke, D. Kruerke, C. Lohning, D. Lotzsch, D. Moro, M. Muller and H. Sawade, *J. Mater. Chem.*, 2000, **10**, 2657-2661.
3 Y. Hisakado, H. Kikuchi, T. Nagamura and T. Kajiyama, *Adv. Mater.*, 2005, **17**, 96-98.
4 H. S. Kitzerow, *Chemphyschem : a European journal of chemical physics and physical chemistry*, 2006, **7**, 63-66.
5 J.-i. Fukuda and S. Zumer, *Phys. Rev. Lett.*, 2010, **104**.
6 A. Mazzulla, G. Petriashvili, M. A. Matranga, M. P. De Santo and R. Barberi, *Soft Matter*, 2012, **8**, 4882-4885.
7 H. Choi, H. Higuchi and H. Kikuchi, *Appl. Phys. Lett.*, 2011, **98**.
8 Y.-H. Lin, H.-S. Chen, H.-C. Lin, Y.-S. Tsou, H.-K. Hsu and W.-Y. Li, *Appl. Phys. Lett.*, 2010, **96**.
9 H. Kikuchi, M. Yokota, Y. Hisakado, H. Yang and T. Kajiyama, *Nat. Mater.*, 2002, **1**, 64-68.
10 F. Castles, F. Day, S. Morris, D. Ko, D. Gardiner, M. Qasim, S. Nosheen, P. Hands, S. Choi and R. Friend, *Nat. Mater.*, 2012, **11**, 599-603.
11 H. Yoshida, Y. Tanaka, K. Kawamoto, H. Kubo, T. Tsuda, A. Fujii, S. Kuwabata, H. Kikuchi and M. Ozaki, *Appl. Phys. Express*, 2009, **2**, 121501.
12 Y. Kogawa, T. Hirose and A. Yoshizawa, *J. Mater. Chem.*, 2011, **21**, 19132-19137.
13 S. Taushanoff, K. Van Le, J. Williams, R. J. Twieg, B. K. Sadashiva, H. Takezoe and A. Jakli, *J. Mater. Chem.*, 2010, **20**, 5893-5898.
14 W. He, G. Pan, Z. Yang, D. Zhao, G. Niu, W. Huang, X. Yuan, J. Guo, H. Cao and H. Yang, *Adv. Mater.*, 2009, **21**, 2050-2053.
15 H. J. Coles and M. N. Pivnenko, *Nature*, 2005, **436**, 997-1000.
16 A. Yoshizawa, Y. Kogawa, K. Kobayashi, Y. Takanishi and J. Yamamoto, *J. Mater. Chem.*, 2009, **19**, 5759-5764.
17 A. Yoshizawa, M. Sato and J. Rokunohe, *J. Mater. Chem.*, 2005, **15**, 3285-3290.
18 M. Lee, S.-T. Hur, H. Higuchi, K. Song, S.-W. Choi and H. Kikuchi, *J. Mater. Chem.*, 2010, **20**, 5813-5816.

19 K. Kishikawa, H. Itoh, S. Akiyama, T. Kobayashi and S. Kohmoto, *J. Mater. Chem.*, 2012, **22**, 8484-8491.

20 T. Kato, J. M. Frechet, P. G. Wilson, T. Saito, T. Uryu, A. Fujishima, C. Jin and F. Kaneuchi, *Chem. mater.*, 1993, **5**, 1094-1100.

21. C. M. Paleos and D. Tsiourvas, *Liq. Cryst.*, 2001, **28**, 1127-1161.

22 I. Noda, *J. Am. Chem. Soc.*, 1989, **111**, 8116-8118.

23 I. Noda, *Appl. spectrosc.*, 1993, **47**, 1329-1336.

24 C.-Y. Fan, H.-C. Jau, T.-H. Lin, F. C. Yu, T.-H. Huang, C. Liu and N. Sugiura, *J. Disp. Technol.*, 2011, **7**, 615-618.

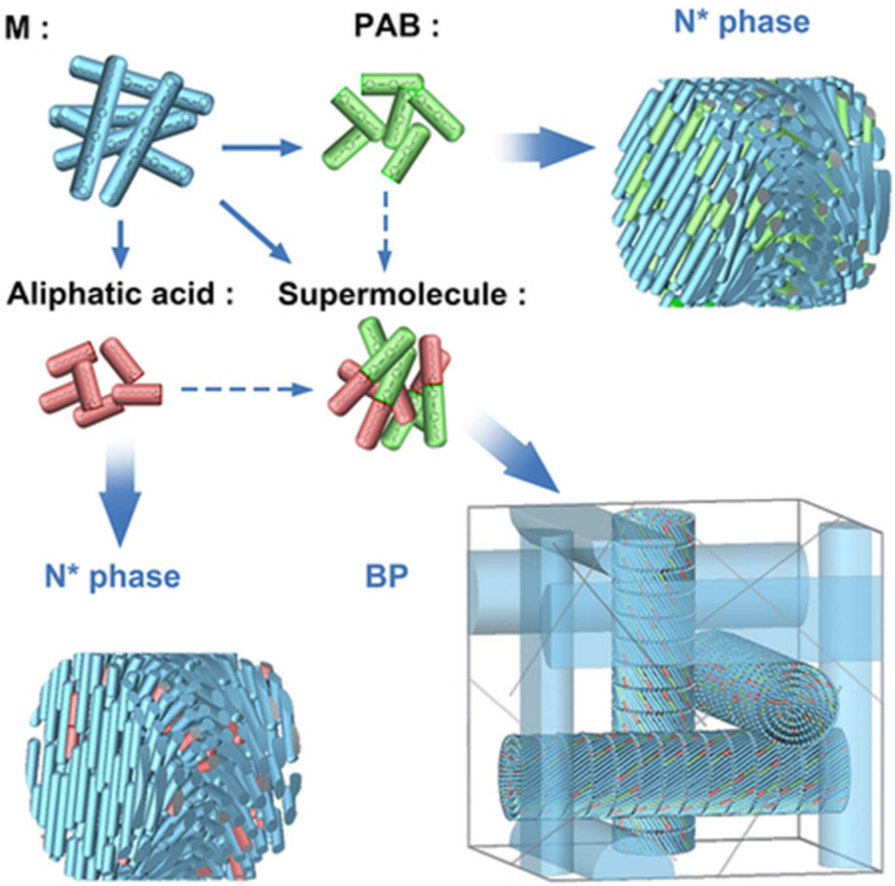

Formation of blue phase induced by rod-shaped hydrogen-bonded supermolecules possessing no chirality or mesomorphic behaviour.
39x38mm (300 x 300 DPI)